

Received: 27.10.2017

Accepted: 07.11.2017

Research Article

## Determination of Inhibition Mechanism of Mono-Azo Naphthylamine Dyes: A Computational Corrosion Study

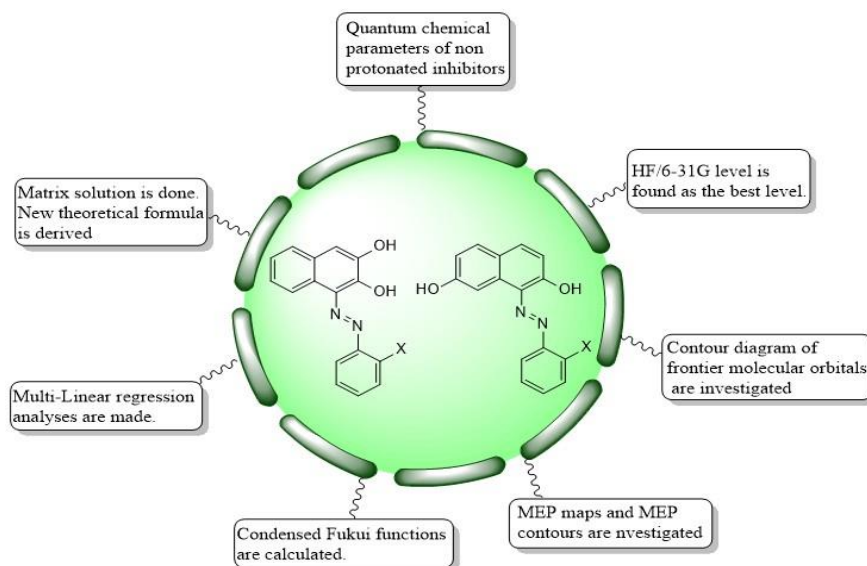
Nihat KARAKUŞ<sup>1</sup>

Department of Chemistry, Faculty of Science, Cumhuriyet University, 58140 Sivas, Turkey

**Abstract:** Some mono azo naphthylamine dyes are optimized by using HF, B3LYP and M062X with 6-31G(d) level in gas phase. The best level is found as HF/6-31G(d) level in gas phase. A well agreement between experimental results and calculated results is found. Contour diagram of frontier molecular orbitals, MEP maps, MEP contours, NBO analyses and Fukui functions are calculated and examined in detail to foresee the corrosion protection mechanism. Regression and matrix analyses are used to derive the new theoretical formula. Experimental and theoretical formula are compared with each other and well agreement is calculated among of them.

**Keywords:** Naphthylamine, Ab-initio, DFT, Molecular Modelling, Quantum Chemical Descriptors.

### Graphical Abstract



- Investigations of anti-corrosive properties are performed by using HF, B3LYP and M062X methods.
- HF/6-31G(d) is found as the best calculation level and it is taken into consideration in other calculations
- Corrosion protection mechanism is predicted by using MEP maps, MEP contours, Fukui functions and contour diagram of FMOs.
- New theoretical formula is derived by multi-linear regression analyses and matrix solution.

<sup>1</sup> Corresponding Author

e-mail: nkarakus@cumhuriyet.edu.tr

## 1. Introduction

Corrosion means the gradual destruction of materials by chemical and/or electrochemical reaction with their environment [1-3]. Controlling and stopping corrosion is so important for industries. Corrosion affects people and industries and their environment. Investigations of anti-corrosive properties, therefore, are important and will continue throughout human life. Large investments are made in this regard and many experiments are carried out. Inhibitors are used in corrosion prevention and their efficiency ranking can be learned by experimental or computational methods [4-12]. Computational research has many advantages and gives important results to experimental works. There are a lot of computational research over corrosion in literature.

Selected mono azo naphthylamine dyes have been synthesized by Mabrouk et al. in 2011 and their corrosion inhibition efficiencies have been investigated toward aluminum in 2M HCl solutions [13]. In their study, weight loss, thermometry and galvanostatic polarization techniques have been used. In this study, mentioned inhibitors are investigated via computational methods. HF, B3LYP and M062X methods are used with 6-31G(d) basis set in calculations. Fully optimizations are carried out and some quantum chemical descriptors are determined. These descriptors are energy of the highest occupied molecular orbital (EHOMO), energy of the lowest unoccupied molecular orbital (ELUMO), energy gap among frontier molecular orbitals (EGap), chemical hardness ( $\eta$ ), chemical softness ( $\sigma$ ), absolute electronegativity ( $\chi$ ), electrophilicity index ( $\omega$ ) and nucleophilicity index (N). These descriptors are often used in foreseeing the inhibition efficiency ranking on inhibitors or reactivity ranking of chemicals. These parameters are calculated from results of optimized structures in each level. Then, experimental inhibition efficiency ranking is compared with calculated results. In this way, the best calculation level is determined. This level is used in the prediction of corrosion mechanism and in the derivation of theoretical formula. In the determination of corrosion mechanism, molecular electrostatic potential (MEP) map, MEP contour, contour diagram of HOMO and LUMO, natural bond

orbital (NBO) analyses and Fukui functions are used. Additionally, the most compatible descriptors are determined by regression analyses.

## 2. Method

Computational investigations of mono azo naphthylamine dyes were performed via Gaussian package program which are Gauss View 5.0.8 [14], Gaussian 09 IA32W-G09RevA.02 [15] and Gaussian 09 AML64-G09RevD.01 [16]. Pre-calculations were done by personal computers and full calculations were carried out via Linux server in TÜBİTAK TR-Grid from TURKEY. Additionally, ChemBioDraw Ultra Version (13.0.0.3015) program was used in preparation of some figures [17]. Hartree-Fock (HF) [18] and hybrid density functional theory (DFT) functionals, B3LYP [19] and M062X [20] methods, was used in calculation with 6-31G(d) basis set. No imaginary frequency was observed in results of calculation. Mentioned quantum chemical descriptors are via Eq. (1) – (9) [21–28]. In calculation of these parameters, Koopmans theorem was taken into account [29]. Fukui functions for nucleophilic attack ( $f_k^+$ ), electrophilic attack ( $f_k^-$ ) and radicalic attack ( $f_k^0$ ) are calculated [30]. For a system of N electron, fully optimizations are performed at the same level of theory for corresponding systems of (N + 1) and (N – 1) electron. The natural population analysis yields to  $P_k(N - 1)$ ,  $P_k(N)$  and  $P_k(N + 1)$ ; the population for all k atoms.

$$I = -E_{HOMO} \quad (1)$$

$$A = -E_{LUMO} \quad (2)$$

$$E_{GAP} = E_{LUMO} - E_{HOMO} \quad (3)$$

$$\eta = \frac{I - A}{2} = \frac{E_{LUMO} - E_{HOMO}}{2} \quad (4)$$

$$\sigma = \frac{1}{\eta} \quad (5)$$

$$\chi = \frac{|I + A|}{2} = \frac{|-E_{HOMO} - E_{LUMO}|}{2} \quad (6)$$

$$CP = -\chi \quad (7)$$

Nihat KARAKUŞ

$$\omega = \frac{CP^2}{2\eta} \quad (8)$$

$$N = \frac{1}{\omega} \quad (9)$$

$$f_k^+ = P_k(N + 1) - P_k(N) \quad (10)$$

$$f_k^- = P_k(N1) - P_k(N - 1) \quad (11)$$

$$f_k^0 = \frac{P_k(N + 1) - P_k(N - 1)}{2} \quad (12)$$

### 3. Results and discussion

#### 3.1. Optimized Geometry

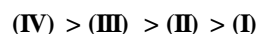
Investigated inhibitors are optimized at HF/6-31G(d), B3LYP/6-31G(d) and M062X/6-31G(d) levels in gas phase. Schematic and optimized structures of studied inhibitors are given in Fig. 1. Calculated quantum chemical descriptors are given in Table 1 at HF/6-31G(d), B3LYP/6-31G(d) and M062X/6-31G(d) levels.

The energy of HOMO is significant descriptors in explanation of anti-corrosion properties of related molecules. The high value of its means that inhibitor may easily coordinate to metal surface by giving electrons. Hence, inhibition efficiency of inhibitors increases with increasing of E<sub>HOMO</sub>. The energy value of LUMO is a descriptor which is used by researcher in determination of inhibition efficiency ranking. Tendency of coordinating increases with the lower energy value of LUMO. Another descriptor is energy gap between frontier molecular orbitals. Electron mobility is important subject in explanation of anti-corrosive properties of inhibitors. Electron mobility increases with decreasing of energy gap. Hence, anti-corrosive properties of inhibitors increase with decreasing of EGAP. In addition to these parameters, chemical hardness and chemical softness is considerable descriptor. Since, metallic bulks are known as chemical soft structure. They prefer to interact with soft molecule. Thence, the increasing of chemical softness increases the inhibition efficiency of molecules. Another parameter is electronegativity. Decreasing of electronegativity implies the increasing of anti-corrosion properties. The last

parameters are electrophilicity and nucleophilicity indexes. Increasing of nucleophilicity index or decreasing of electrophilicity index increases the coordination tendency of inhibitor against metallic surface. Therefore, it is expected that inhibition efficiency increases with increasing of nucleophilicity index. According to above explanations, inhibition efficiency ranking for each descriptor should be as follow.

According to E <sub>HOMO</sub>	<b>(IV) &gt; (III) &gt; (II) &gt; (I)</b> (HF)
	<b>(IV) &gt; (III) &gt; (II) &gt; (I)</b> (B3LYP)
	<b>(IV) &gt; (III) &gt; (II) &gt; (I)</b> (M062X)
According to E <sub>LUMO</sub>	<b>(III) &gt; (IV) &gt; (II) &gt; (I)</b> (HF)
	<b>(II) &gt; (I) &gt; (IV) &gt; (III)</b> (B3LYP)
	<b>(II) &gt; (I) &gt; (IV) &gt; (III)</b> (M062X)
According to E <sub>GAP</sub>	<b>(IV) &gt; (III) &gt; (II) &gt; (I)</b> (HF)
	<b>(II) &gt; (I) &gt; (IV) &gt; (III)</b> (B3LYP)
	<b>(II) &gt; (I) &gt; (IV) &gt; (III)</b> (M062X)
According to η and σ	<b>(IV) &gt; (III) &gt; (II) &gt; (I)</b> (HF)
	<b>(II) &gt; (I) &gt; (IV) &gt; (III)</b> (B3LYP)
	<b>(II) &gt; (I) &gt; (IV) &gt; (III)</b> (M062X)
According to χ	<b>(IV) &gt; (III) &gt; (I) &gt; (II)</b> (HF)
	<b>(IV) &gt; (III) &gt; (I) &gt; (II)</b> (B3LYP)
	<b>(IV) = (III) &gt; (I) &gt; (II)</b> (M062X)
According to ω and N	<b>(IV) &gt; (III) &gt; (I) &gt; (II)</b> (HF)
	<b>(III) &gt; (IV) &gt; (II) = (I)</b> (B3LYP)
	<b>(III) &gt; (IV) &gt; (I) &gt; (II)</b> (M062X)

According to above ranking the most compatible ranking is obtained at HF/6-31G(d) level in the gas phase. Hence, this level is taken into account for other calculations. Additionally, calculated general inhibition efficiency ranking is found as follow:



Above ranking is in agreement with experimental results. In addition to this result, it is found that electron releasing group (-OCH<sub>3</sub>) increases the inhibition efficiency of inhibitor while electron donating group (-COOH) decreases the inhibition efficiency of inhibitors.

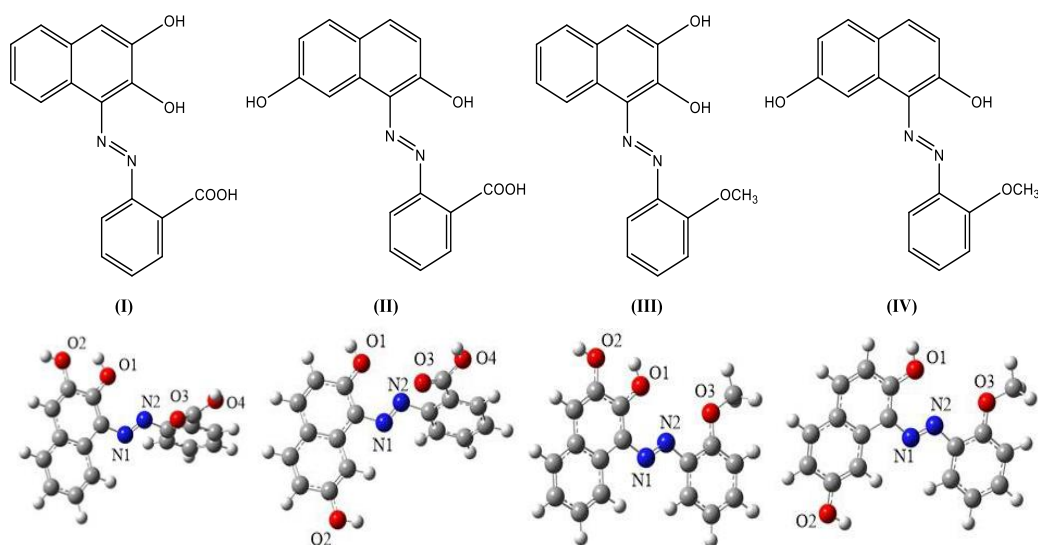


**Fig. 1.** Schematic and optimized structures of studied mono azo naphthylamine dyes at HF/6-31G(d) level in gas phase.

**Table 1.** Calculated descriptors for inhibitor (I) – (IV) at related levels in gas phase

Inhibitors	$E_{\text{HOMO}}^1$	$E_{\text{LUMO}}^1$	$E_{\text{GAP}}^1$	$\eta^1$	$\sigma^2$	$\chi^1$	$\omega^1$	$N^2$
HF/6-31G(d)								
Inhibitor (I)	-7.614	2.039	9.653	4.827	0.207	2.788	0.805	1.242
Inhibitor (II)	-7.602	1.974	9.575	4.788	0.209	2.814	0.827	1.209
Inhibitor (III)	-7.325	1.932	9.257	4.629	0.216	2.696	0.785	1.273
Inhibitor (IV)	-7.303	1.946	9.249	4.624	0.216	2.679	0.776	1.289
B3LYP/6-31G(d)								
Inhibitor (I)	-5.510	-2.218	3.292	1.646	0.607	3.864	4.536	0.220
Inhibitor (II)	-5.495	-2.221	3.274	1.637	0.611	3.858	4.545	0.220
Inhibitor (III)	-5.223	-1.887	3.337	1.668	0.599	3.555	3.787	0.264
Inhibitor (IV)	-5.204	-1.890	3.314	1.657	0.604	3.547	3.797	0.263
M062X/6-31G(d)								
Inhibitor (I)	-6.757	-1.282	5.475	2.737	0.365	4.019	2.951	0.339
Inhibitor (II)	-6.742	-1.306	5.436	2.718	0.368	4.024	2.978	0.336
Inhibitor (III)	-6.518	-0.983	5.535	2.768	0.361	3.750	2.541	0.394
Inhibitor (IV)	-6.497	-1.002	5.495	2.747	0.364	3.750	2.559	0.391

<sup>1</sup> in eV, <sup>2</sup> in eV<sup>-1</sup>

**Table 2.** Calculated quantum chemical descriptors of inhibitor (I) – (IV) at HF/6-31G(d) level in aqua

Inhibitors	$E_{\text{HOMO}}^1$	$E_{\text{LUMO}}^1$	$E_{\text{GAP}}^1$	$\eta^1$	$\sigma^2$	$\chi^1$	$\omega^1$	$N^2$
Inhibitor (I)	-7.913	1.668	9.582	4.791	0.209	3.122	1.018	0.983
Inhibitor (II)	-7.763	1.310	9.074	4.537	0.220	3.226	1.147	0.872
Inhibitor (III)	-7.662	1.522	9.184	4.592	0.218	3.070	1.026	0.974
Inhibitor (IV)	-7.596	1.597	9.193	4.597	0.218	3.000	0.979	1.022

<sup>1</sup> in eV, <sup>2</sup> in eV<sup>-1</sup>

### 3.2. Optimization of Inhibitors in Aqua

Investigated compounds are re-optimized at HF/6-31G(d) level in aqua. Related quantum chemical descriptors are re-calculated and given in Table 2.

In terms of quantum chemical descriptors in Table 2, inhibition efficiency ranking of related compounds should be given as follow:

According to $E_{HOMO}$	(IV) > (III) > (II) > (I)
According to $E_{LUMO}$	(II) > (III) > (IV) > (I)
According to $E_{GAP}$	(II) > (III) > (IV) > (I)
According to $\eta$ and $\sigma$	(II) > (III) > (IV) > (I)
According to $\chi$	(IV) > (III) > (I) > (II)
According to $\omega$ and N	(IV) > (I) > (III) > (II)

Results in aqua show that these calculations are inadequate in explanation of the anti-corrosion properties. It is determined that computational investigations in water is not appropriate for our studied molecules.

### 3.3. Prediction of Corrosion Mechanism

The most important stage in corrosion research is determination of corrosion mechanism. If mechanism is determined close to truth, it may be easier to recommend the inhibition efficiency and the anti-corrosive molecules. The first one is contour diagram of frontier molecular orbital and they are represented in Fig. 2.

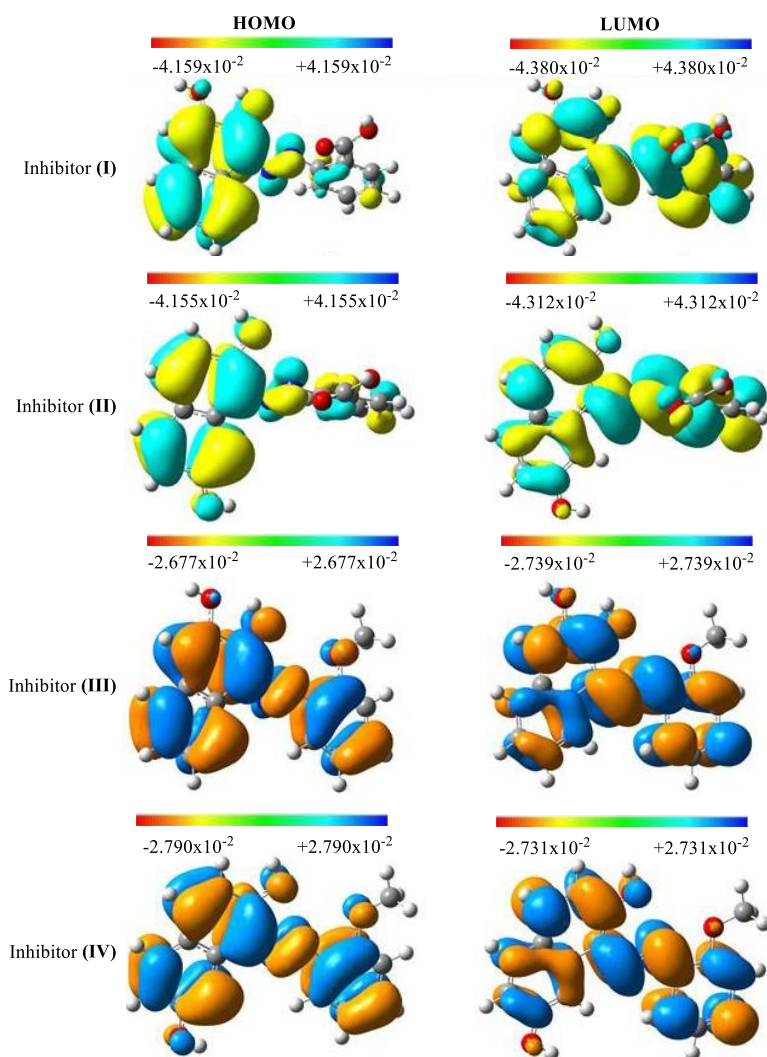
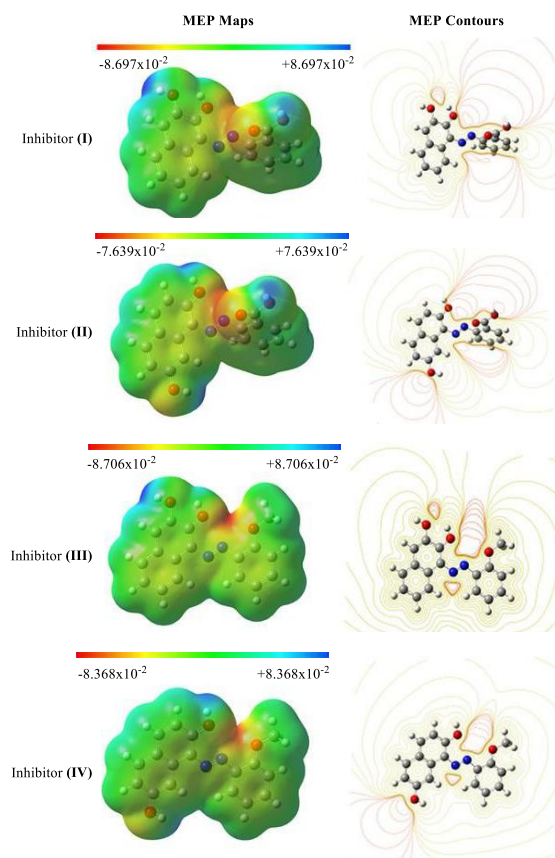


Fig. 2. Contour diagram of frontier molecular orbitals of related compounds at HF/6-31G(d) level in gas phase.

According to Fig. 2, if molecule gives electrons to the metal surface, they belong to HOMO and these electrons are mainly delocalized on the molecule surface. These results showed that  $\pi$  electrons have a significant effect on corrosion protection. Additionally, electron density at HOMO of inhibitor (III) and (IV) is more than those of inhibitor (I) and (II). It is expected that corrosion inhibition efficiency of (III) and (IV) is better than those of inhibitor (I) and (II). As for the contour diagram of LUMO, if studied compounds accept electron from metal, these electrons will be mainly delocalized on the structure. The other part to be examined is MEP maps and contours. They calculated at HF/6-31G(d) level in gas phase and represented in Fig. 3.

According to Fig. 3, the reactivity of heteroatoms is not as much as expected. Because there are not so many red or yellow regions in the environment of heteroatoms. Additionally, it is easily seen that the steric effects are dominant in the environment of heteroatoms. In determination of corrosion mechanism, molecular structure is so important. If

optimized structures are examined in detail, molecular planarity in inhibitor (III) and (IV) is more than those of others. It is understood that surface area among related inhibitors and metal is more than those of others. Also, inhibition efficiencies of inhibitor (III) and (IV) are better than those of inhibitor (I) and (II). The other important stage is the determination of corrosion mechanism is NBO analyses. The stabilization energy of the second order perturbation theory is mainly associated with delocalization. Lower stabilization energy is mean that better inhibition efficiency. The lowest stabilization energy is calculated as -506.27, -2057.92, -530.24 and -453.69 kcal mol<sup>-1</sup> for inhibitor (I) – (IV), respectively. According to these results, it is expected that inhibitor (IV) is the best corrosion inhibitor. The last one is Fukui functions for electrophilic, nucleophilic and radicalic attacks. Fukui functions are calculated at HF/6-31G(d) level in gas phase via using Eq. (10) – (12) and they are given in Table 3 for heteroatoms.



**Fig. 3.** MEP maps and contours of investigated chemicals at HF/6-31G(d) level in vacuum.

**Table 3.** Calculated condensed Fukui functions for heteroatom in mentioned molecules

Inhibitors	Atoms	$P_k(N+1)$	$P_k(N)$	$P_k(N-1)$	$f_k^+$	$f_k^0$	$f_k^-$
Inhibitor (I)	N1	7.434	7.191	7.105	0.24292	0.16463	0.08634
	N2	7.397	7.129	6.738	0.26769	0.329545	0.39140
	O1	8.735	8.737	8.748	-0.00218	-0.00693	-0.01167
	O2	8.789	8.771	8.765	0.01749	0.01178	0.00607
	O3	8.748	8.681	8.683	0.06744	0.03251	-0.00242
	O4	8.756	8.782	8.761	-0.02524	-0.00225	0.02074
Inhibitor (II)	N1	7.426	7.190	7.109	0.23628	0.15884	0.08140
	N2	7.407	7.143	6.744	0.26375	0.33169	0.39963
	O1	8.726	8.726	8.747	0.00018	-0.01036	-0.0209
	O2	8.769	8.745	8.734	0.02369	0.01757	0.01145
	O3	8.750	8.681	8.685	0.06873	0.03268	-0.00337
	O4	8.756	8.782	8.761	-0.02591	-0.00241	0.02109
Inhibitor (III)	N1	7.476	7.224	7.107	0.25161	0.18440	0.11719
	N2	7.348	7.134	6.755	0.21450	0.296435	0.37837
	O1	8.732	8.718	8.746	0.01448	-0.00699	-0.02847
	O2	8.787	8.773	8.765	0.01422	0.01092	0.00762
	O3	8.589	8.587	8.605	0.00184	-0.00783	-0.01750
Inhibitor (IV)	N1	7.466	7.218	7.108	0.24792	0.17882	0.10972
	N2	7.361	7.147	6.762	0.21373	0.29922	0.38471
	O1	8.723	8.710	8.745	0.01281	-0.01110	-0.03500
	O2	8.771	8.746	8.734	0.02504	0.01843	0.01182
	O3	8.590	8.588	8.606	0.00178	-0.00809	-0.01797

According to Table 3, N2 atom is appropriate for electrophilic, nucleophilic and radicalic attacks in inhibitor (I) and (II) while N1, N2 ve N2 atoms is appropriate for nucleophilic, radicalic and electrophilic attacks, respectively in inhibitor (III) and (IV).

As a result, The N1 and N2 atoms are in the interior of the molecules and sterically crowded. Thence, it is thought that inhibitors will protect the metal horizontally rather than a single point. Also, due to their planarity, inhibition efficiencies of inhibitor (III) and (IV) are better than those of (I) and (II). In terms of NBO analysis, inhibitor (IV) is the best molecule in protection of metal in corrosion. All these results are appropriate with experimental results. The inhibitors cover the surface of the metal horizontally.

### 3.4. Regression Analyses and Theoretical Formula

Regression analyses is important step in search of harmony between experimental and calculated results. The scatter graphs are plotted by using experimental inhibition efficiencies and quantum chemical parameters. These graphs are represented in Supp. Fig. S1 – S6 for each quantum chemical descriptors, respectively. According to these

graphs,  $E_{HOMO}$ ,  $E_{LUMO}$ ,  $E_{GAP}$  and chemical softness are the most compatible descriptors. They are used to derived new theoretical formula for derivatives of mono azo naphthylamine dyes. This formula is given in Eq. (13).

$$\%IE_{Teorik} = 5504.34 \times E_{HOMO} + 5599.49 \times E_{LUMO} - 5530.34 \times E_{GAP} + 666.49 \times \sigma \quad (13)$$

Eq. (13) is obtained by regression analysis and matrix solution. Experimental inhibition efficiencies of inhibitor (I) – (IV) have been reported as 81.08, 83.76, 87.19 and 88.73, respectively while they calculated as 81.00, 83.68, 87.11 and 88.65, respectively. The scatter graph is plotted by using these values and represented in Fig. 4.

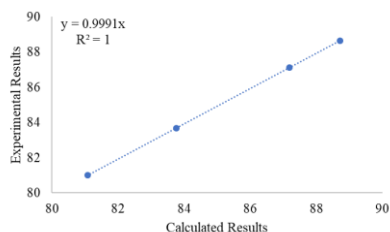


**Fig. 4.** The scatter graph between experimental and calculated inhibition efficiencies.

According to Fig. 4, correlation coefficient ( $R^2$ ) indicates the orientation between the experimental and calculated results. The orientation is good for our studied molecules. The agreement between related results can be handled by graphic slope. Graphic slope of our graphic is calculated as 0.9991. It indicates that, there is a well agreement between experimental and calculated results.

#### 4. Conclusion

Studied mono azo naphthylamine compounds are optimized at HF/6-31G(d), B3LYP/6-31G(d) and M062X/6-31G(d) levels in gas phase. Quantum chemical descriptors of mentioned molecules are calculated in each level and compared with experimental ones. The best method is determined as HF/6-31G(d) level and this level is taken into consideration in calculation of MEP maps, MEP contours, HOMO and LUMO contour diagram, NBO calculations, optimization in water and condensed Fukui functions. All quantum chemical parameters are compared with experimental inhibition efficiency and compatible descriptors are determined by regression analyses. Then, a new theoretical formula for aluminum is derived by matrix solution. The well agreement is calculated between experimental and calculated inhibition efficiencies.

#### Acknowledgment

This work is supported by the Scientific Research Project Fund of Cumhuriyet University under the project number F-490. This research is made possible by TUBITAK ULAKBIM, High Performance and Grid Computing Center (TR-Grid e-Infrastructure).

#### References

- [1] Yuxi Zhao, Xiaowen Zhang, Weiliang Jin, Influence of environment on the development of corrosion product-filled paste and a corrosion layer at the steel/concrete interface, Corrosion Science <http://dx.doi.org/10.1016/j.corsci.2017.03.026>.
- [2] D.-H. Xia, et al., Atmospheric corrosion assessed from corrosion images using fuzzy Kolmogorov–Sinai entropy, Corros. Sci. (2017), <http://dx.doi.org/10.1016/j.corsci.2017.02.015>.
- [3] N.D. Alexopoulos, et al., Synergy of corrosion-induced micro-cracking and hydrogen embrittlement on the structural integrity of aluminium alloy (Al-Cu-Mg) 2024, Corros. Sci. (2017), <http://dx.doi.org/10.1016/j.corsci.2017.03.001>.
- [4] Jinlong Wang, Minghui Chen, Yuxian Cheng, Lanlan Yang, Zebin Bao, Li Liu, Shenglong Zhu, Fuhui Wang, Hot corrosion of arc ion plating NiCrAlY and sputtered nanocrystalline coatings on a nickel-based single-crystal superalloy, Corrosion Science <http://dx.doi.org/10.1016/j.corsci.2017.04.004>.
- [5] Yuxi Zhao, Xiaowen Zhang, Weiliang Jin, Influence of environment on the development of corrosion product-filled paste and a corrosion layer at the steel/concrete interface, Corrosion Science <http://dx.doi.org/10.1016/j.corsci.2017.03.026>.
- [6] L. Wei, et al., Effect of exposure angle on the corrosion behavior of X70 steel under supercritical CO<sub>2</sub> and gaseous CO<sub>2</sub> environments, Corros. Sci. (2017), <http://dx.doi.org/10.1016/j.corsci.2017.03.011>.
- [7] Y. Han, et al., Effects of electropolishing on corrosion and stress corrosion cracking of Alloy 182 in high temperature water, Corros. Sci. (2017), <http://dx.doi.org/10.1016/j.corsci.2017.03.004>.
- [8] T.J. Watson, et al., Salt fog corrosion behavior in a powder-processed icosahedral-phase-strengthened aluminum alloy, Corros. Sci. (2017), <http://dx.doi.org/10.1016/j.corsci.2017.03.010>.
- [9] H.N. Krogstad, R. Johnsen, Corrosion properties of nickel-aluminium bronze in natural seawater—Effect of galvanic coupling to UNS S31603, Corros. Sci. (2017), <http://dx.doi.org/10.1016/j.corsci.2017.03.016>.
- [10] Xianghong Li, Shuduan Deng, Tong Lin, Xiaoguang Xie, Guanben Du, 2-Mercaptopyrimidine as an effective inhibitor for the corrosion of cold rolled steel in HNO<sub>3</sub> solution, Corrosion Science 118 (2017) 202–216.

- [11] Y. Qiang, et al., Experimental and theoretical studies of four allyl imidazolium-based ionic liquids as green inhibitors for copper corrosion in sulfuric acid, *Corros. Sci.* (2017), <http://dx.doi.org/10.1016/j.corsci.2017.02.021>.
- [12] Zohreh Salarvand, Mehdi Amirasr, Milad Talebian, Keyvan Raeissi, Soraia Meghdadi, Enhanced corrosion resistance of mild steel in 1 M HCl solution by trace amount of 2-phenyl-benzothiazole derivatives: Experimental, quantum chemical calculations and molecular dynamics (MD) simulation studies, *Corrosion Science* 114 (2017) 133–145.
- [13] .M. Mabrouk, H. Shokry, K. M. Abu Al-Naja, Inhibition of aluminum corrosion in acid solution by mono- and bis-azo naphthylamine dyes. Part 1, *Chem Met Alloys* 4 (2011) 98–106.
- [14] GaussView, Version 5, Roy Dennington, Todd Keith, and John Millam, Semichem Inc., Shawnee Mission, KS, 2009.
- [15] Gaussian 09, Revision A.02, M. J. Frisch, G. W. Trucks, H. B. Schlegel, G. E. Scuseria, M. A. Robb, J. R. Cheeseman, G. Scalmani, V. Barone, B. Mennucci, G. A. Petersson, H. Nakatsuji, M. Caricato, X. Li, H. P. Hratchian, A. F. Izmaylov, J. Bloino, G. Zheng, J. L. Sonnenberg, M. Hada, M. Ehara, K. Toyota, R. Fukuda, J. Hasegawa, M. Ishida, T. Nakajima, Y. Honda, O. Kitao, H. Nakai, T. Vreven, J. A. Montgomery, Jr., J. E. Peralta, F. Ogliaro, M. Bearpark, J. J. Heyd, E. Brothers, K. N. Kudin, V. N. Staroverov, R. Kobayashi, J. Normand, K. Raghavachari, A. Rendell, J. C. Burant, S. S. Iyengar, J. Tomasi, M. Cossi, N. Rega, J. M. Millam, M. Klene, J. E. Knox, J. B. Cross, V. Bakken, C. Adamo, J. Jaramillo, R. Gomperts, R. E. Stratmann, O. Yazyev, A. J. Austin, R. Cammi, C. Pomelli, J. W. Ochterski, R. L. Martin, K. Morokuma, V. G. Zakrzewski, G. A. Voth, P. Salvador, J. J. Dannenberg, S. Dapprich, A. D. Daniels, Ö. Farkas, J. B. Foresman, J. V. Ortiz, J. Cioslowski, and D. J. Fox, Gaussian, Inc., Wallingford CT, 2009.
- [16] Gaussian 09, Revision D.01, M. J. Frisch, G. W. Trucks, H. B. Schlegel, G. E. Scuseria, M. A. Robb, J. R. Cheeseman, G. Scalmani, V. Barone, B. Mennucci, G. A. Petersson, H. Nakatsuji, M. Caricato, X. Li, H. P. Hratchian, A. F. Izmaylov, J. Bloino, G. Zheng, J. L. Sonnenberg, M. Hada, M. Ehara, K. Toyota, R. Fukuda, J. Hasegawa, M. Ishida, T. Nakajima, Y. Honda, O. Kitao, H. Nakai, T. Vreven, J. A. Montgomery, Jr., J. E. Peralta, F. Ogliaro, M. Bearpark, J. J. Heyd, E. Brothers, K. N. Kudin, V. N. Staroverov, R. Kobayashi, J. Normand, K. Raghavachari, A. Rendell, J. C. Burant, S. S. Iyengar, J. Tomasi, M. Cossi, N. Rega, J. M. Millam, M. Klene, J. E. Knox, J. B. Cross, V. Bakken, C. Adamo, J. Jaramillo, R. Gomperts, R. E. Stratmann, O. Yazyev, A. J. Austin, R. Cammi, C. Pomelli, J. W. Ochterski, R. L. Martin, K. Morokuma, V. G. Zakrzewski, G. A. Voth, P. Salvador, J. J. Dannenberg, S. Dapprich, A. D. Daniels, Ö. Farkas, J. B. Foresman, J. V. Ortiz, J. Cioslowski, and D. J. Fox, Gaussian, Inc., Wallingford CT, 2009.
- [17] PerkinElmer, 2012. ChemBioDraw Ultra Version (13.0.0.3015), CambridgeSoft Waltham, MA, USA.
- [18] C. C. J. Roothaan, New Developments in Molecular Orbital Theory, *Rev Mod Phys* 23 (1951) 69.
- [19] A. D. Becke, Density-functional thermochemistry. III. The role of exact exchange, *J Chem Phys* 98 (1993) 5648-5652.
- [20] Y. Zhao, D. G. Truhlar, The M06 suite of density functionals for main group thermochemistry, thermochemical kinetics, noncovalent interactions, excited states, and transition elements: Two new functionals and systematic testing of four M06-class functionals and 12 other functionals". *Theor Chem Account* 120 (2006) 215–241.
- [21] K. Sayin, S. E. Kariper, T. A. Sayin, D. Karakaş, Theoretical spectroscopic study of seven zinc (II) complex with macrocyclic Schiff-base ligand. *Spectrochimica Acta Part A: Molecular and Biomolecular Spectroscopy* 133 (2014) 348-356.
- [22] S. G. Sagdinc, D. Erdas, I. Gunduz, A. E. Sahinturk, FT-IR and FT-Raman spectra, molecular structure and first-order molecular hyperpolarizabilities of a potential antihistaminic drug, cyproheptadine HCl. *Spectrochimica Acta Part A: Molecular*

- and Biomolecular Spectroscopy 134 (2015) 350-360.
- [23] A. A. Soayed, A. F. El-Husseiny, Potentiometry and geometrical structure of some azodye compounds and their metal complexes. *Journal of Molecular Liquids* 209 (2015) 258-266.
- [24] W. H. Mahmoud, N. F. Mahmoud, G. G. Mohamed, A. A. El-Bindary, A. Z. El-Sonbati, Supramolecular structural, thermal properties and biological activity of 3-(2-methoxyphenoxy) propane-1, 2-diol metal complexes. *Journal of Molecular Structure* 1086 (2015) 266-275.
- [25] A. Z. El-Sonbati, M. A. Diab, A. A. El-Bindary, M. M. Ghoneim, M. T. Mohesien, M. A. El-Kader, Polymeric complexes—LXI. Supramolecular structure, thermal properties, SS-DNA binding activity and antimicrobial activities of polymeric complexes of rhodanine hydrazone compounds. *Journal of Molecular Liquids* 215 (2016) 711-739.
- [26] A. A. El-Bindary, M. M. Ghoneim, M. A. Diab, A. Z. El-Sonbati, L. S. Serag, Thermodynamic studies of N-allylrhodanine derivatives and their metal complexes. *Journal of Molecular Liquids* 223 (2016) 448-461.
- [27] K. Sayin, N. Kurtoglu, M. Kose, D. Karakas, M. Kurtoglu, Computational and experimental studies of 2-[(E)-hydrazinylidenemethyl]-6-methoxy-4-[(E)-phenyldiazenyl] phenol and its tautomers. *Journal of Molecular Structure* 1119 (2016) 413-422.
- [28] Ayhan Üngördü, Nurten Tezer, The solvent (water) and metal effects on HOMO-LUMO gaps of guanine base pair: A computational study, *Journal of Molecular Graphics and Modelling* <http://dx.doi.org/10.1016/j.jmgm.2017.04.015>.
- [29] T Koopmans, Über die Zuordnung von Wellenfunktionen und Eigenwerten zu den Einzelnen Elektronen Eines Atoms, *Physica* 1 (1934) 104–113.
- [30] Nihat Karakus, Koray Sayin, The investigation of corrosion inhibition efficiency on some benzaldehyde thiosemicarbazones and their thiole tautomers: Computational study, *Journal of the Taiwan Institute of Chemical Engineers* 48 (2015) 95–102.